

See discussions, stats, and author profiles for this publication at: <https://www.researchgate.net/publication/3886566>

# Fingerprint image ridge frequency estimation by higher order spectrum

**Conference Paper** in *Proceedings / ICIP ... International Conference on Image Processing* · February 2000

DOI: 10.1109/ICIP.2000.900995 · Source: IEEE Xplore

---

CITATIONS

10

---

READS

324

1 author:



[Xudong Jiang](#)

Nanyang Technological University

142 PUBLICATIONS 3,439 CITATIONS

SEE PROFILE

Some of the authors of this publication are also working on these related projects:



Face Recognition by Sparse Coding [View project](#)

# Fingerprint Image Ridge Frequency Estimation by Higher Order Spectrum

Xudong Jiang

Centre for Signal Processing, Nanyang Technological University

[exdjiang@ntu.edu.sg](mailto:exdjiang@ntu.edu.sg)

## Abstract

*This paper proposes a new approach for estimating the ridgeline frequency of fingerprint images by using higher order spectrum. The higher order spectrum enhances the fundamental frequency component of the ridgeline by using its harmonics and therefore suppresses the noise. A specific form of higher order spectrum other than the traditional bispectrum or trispectrum is employed to improve the reliability of the fingerprint ridge frequency estimation. This approach provides a reliable ridgeline frequency estimation for heavy noised fingerprint images. Experimental results are presented to compare this approach with the traditional approaches of power spectrum, bispectrum and trispectrum.*

## 1. Introduction

Fingerprint image consists of oriented narrow ridges separated by narrow valleys. The local ridge orientation and ridge frequency are two intrinsic features of a fingerprint image. Ridge frequency or ridgeline density is a measure quantifying the number of ridges per unit area, which is a key parameter for an effective fingerprint image processing. O'Gorman and Nickerson [1] and Mehtre [2] performed fingerprint image enhancement by using band pass filters. A. K. Jain, L. Hong, R. Bolle [3, 4] detected ridges with two masks, which in principle perform some kinds of band pass filtering. L. Hong, Y. Wan and A. K. Jain [5] introduced a fingerprint image enhancement method that employed a Gabor filter. However, these image processing algorithms based on the oriented band pass filter may result in ridge location errors and spurious ridge structures if the ridge frequency is not correctly estimated before the filter design. The performance of applying band pass filters to the fingerprint image processing strongly relies on the accuracy of the ridge frequency estimation. Therefore, reliably estimating the ridge frequency is very useful for the effective processing of fingerprint images.

L. Hong, Y. Wan and A. K. Jain estimated the ridge frequency by counting the average number of pixels between two consecutive peaks of gray levels along a direction normal to the local ridge orientation [5]. This is a fast method. However, for a heavy noised image, it is difficult to reliably detect the consecutive peaks of gray levels in the space domain. D. Maio and D. Maltoni proposed an approach to calculate the ridge frequency based on the partial derivatives of sinusoidal signals, which allows the local frequency of sinusoidal signals to be estimated with good accuracy [6]. However, many fingerprint images cannot be modeled by sinusoidal waves. Spectrum analysis techniques enhance the signal and press the noise in the frequency domain if the signal has a narrow frequency band and noise has a wide frequency band. Therefore, heavy noised signal can be more easily and reliably detected in the frequency domain.

Fingerprint gray levels along a direction normal to the local ridge orientation form a well-defined period signal adding noise. If this period signal is not sinusoid shaped its energy is distributed to its fundamental frequency and harmonics. Properly defined higher order spectrum (HOS) can enhance the fundamental frequency component by using the harmonics and therefore suppress noise. However, some periodic non-sinusoidal signals have no even harmonics or have no certain odd harmonic. This will result in failure of employment of the bispectrum or trispectrum. Therefore, we employed another form of higher order spectrum called mix-spectrum [10] for the ridge frequency estimation of fingerprint image.

## 2. Power spectrum of $x$ -signature of the ridges and valleys

Let  $g(i, j)$  be the gray value of a fingerprint image at pixel  $(i, j)$  and  $\phi(i, j)$  be the orientation at this pixel. The orientation  $\phi(i, j)$  represents the ridgeline local orientation at pixel  $(i, j)$  and can be computed using one of the several methods proposed in the literature. We incorporate the method in [3], which uses gradient and least-square methods to estimate the ridge orientation.

Given a pixel  $(i, j)$ , we determine an oriented window of size  $L \times W$  ( $33 \times 7$ ) that is defined in the ridge coordinate system (Fig. 1) and compute the  $x$ -signature  $x[k]$  as in [1], where

$$x[k] = \frac{1}{W} \sum_{d=0}^{W-1} g(u, v), \quad k = 0, 1, \dots, L-1, \quad (1)$$

$$u = i + \left(d - \frac{W}{2}\right) \cos \mathbf{j}(i, j) + \left(k - \frac{L}{2}\right) \sin \mathbf{j}(i, j), \quad (2)$$

$$v = j + \left(d - \frac{W}{2}\right) \sin \mathbf{j}(i, j) + \left(\frac{L}{2} - k\right) \cos \mathbf{j}(i, j). \quad (3)$$

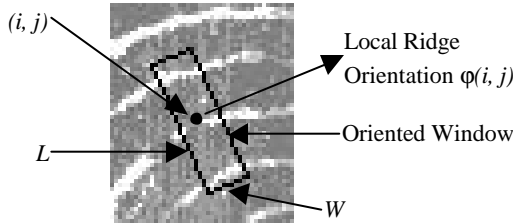


Fig. 1. Oriented window.

The  $x$ -signature forms a period signal adding noise. Fig. 2 illustrates the  $x$ -signature (a) obtained from Fig. 1 and its power spectrum (b). It is seen from Fig. 2(a) that the  $x$ -signature of ridges and valleys is not a sinusoidal-shape signal. For a nonsinusoidal period signal its power is distributed to its fundamental frequency and harmonics. From Fig. 2(b) the fundamental frequency and the second and third harmonics can be clearly identified.

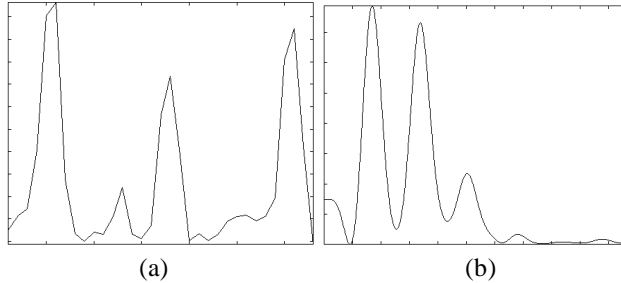


Fig. 2. X-signature (a) obtained from Fig.1 and its power spectrum (b).

Due to the distribution of the signal power, the fundamental frequency component of the power spectrum may be much weaker than that of sinusoidal signal with the same power. Therefore, for a given signal-to-noise ratio (SNR) a nonsinusoidal signal will much more likely be masked by noise than a sinusoidal signal. Furthermore, the noise may have the harmonic components of power spectrum higher than the fundamental component. This will result in a false frequency estimation. In order to solve these problems we use the higher order spectrum to enhance the fundamental frequency component of the spectrum.

### 3. Frequency estimation by HOS

Let  $X(f)$  be the Fourier transform of the  $x$ -signature  $x[k]$  obtained by equation (1). The power spectrum is then given by

$$P(f) = X(f)X^*(f). \quad (4)$$

Some higher order spectrum techniques (bispectrum and trispectrum) [7,8] can be used to enhance the fundamental frequency component. The diagonal slice of bispectrum is defined as

$$B(f) = X(f)X(f)X^*(2f), \quad (5)$$

where  $X(f)$  is the Fourier transform of signal. The diagonal slice of trispectrum is defined as

$$T(f) = X(f)X(f)X(f)X^*(3f). \quad (6)$$

It is clear from the definitions of the bispectrum and trispectrum that they enhance the fundamental frequency component of spectrum by using the second or third harmonic, respectively. They were successfully applied to detect weak signal from the noise [9]. However, even harmonics or the third harmonic may not exist in some periodic signals. This will result in the failure of employment of the bispectrum or trispectrum. For the ridge frequency estimation, the choice of bispectrum or trispectrum is then difficult because of an unknown signal form. Furthermore, the bispectrum and trispectrum may also enhance the noise. For example, the spectrum components at frequencies of a half or one third of the fundamental frequency are strongly enhanced by bispectrum or trispectrum, respectively.

Therefore, we employ another higher order spectrum form, called mix-spectrum [10], defined as follows

$$M(f) = P(f) \min\{\alpha |X(f)|, \max\{|X(2f)|, |X(3f)|\}\}, \quad (7)$$

where  $\min\{\bullet, \bullet\}$  is a minimum operator,  $\max\{\bullet, \bullet\}$  is a maximum operator and  $\alpha$  is a constant ( $0.5 < \alpha < 1.5$ ). In this work, we choose the value of  $\alpha$  to be 1.2.

It is unlikely that the  $x$ -signature of fingerprint image has zero values of amplitude spectrum at both the second and the third harmonic frequencies. Therefore, the mix-spectrum can work well even if the  $x$ -signature has no even harmonics or has no third harmonic. The minimum operator used in (7) is aimed at reducing the side effect of the higher order spectrum. Because the fundamental frequency component of amplitude spectrum is often greater than its harmonics,  $|X(2f)|$  or  $|X(3f)|$  is unlikely harmonic if it is much greater than  $|X(f)|$ . The mix-spectrum enhances the spectrum component at frequency  $f$  maximally by a factor of  $\alpha |X(f)|$ . In this way, the mix-spectrum limits the enhancement of the noise components at frequency  $f$  where  $|X(2f)|$  or  $|X(3f)|$  is greater than  $\alpha |X(f)|$ . Therefore, the mix-spectrum enhances the signal spectrum at the fundamental frequency and suppresses

noise in the presence of either the second or the third harmonic.

Fig. 3 and Fig. 4 illustrate the power spectrum, bispectrum, trispectrum and mix-spectrum of two -6 dB noised rectangular pulse trains of length  $L=64$  with period of  $T=L/4=16$ . The pulse width  $tw$  is  $T/3$  for Fig.3 and  $T/2$  for Fig.4. The DC component of signal was removed before Fourier transform and the maximal peaks of all spectrums were normalized to one. The fundamental frequencies of these signals are  $1/16=0.0625$ . The dotted lines in the figures show the fundamental frequency, the second harmonic and the third harmonic. The estimated values of fundamental frequency by power spectrum  $fp$ , bispectrum  $fb$ , trispectrum  $ft$  and mix-spectrum  $fm$  are given in the figures.

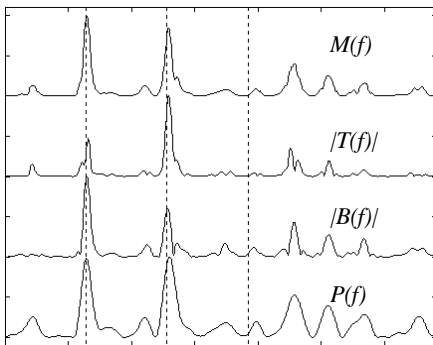


**Fig. 3.** Various spectrums of noised rectangular pulse train with  $tw=T/3$ . The estimated fundamental frequency is:  $fp=0.1269$ ,  $fb=0.0635$ ,  $ft=0.1265$ ,  $fm=0.0629$ .

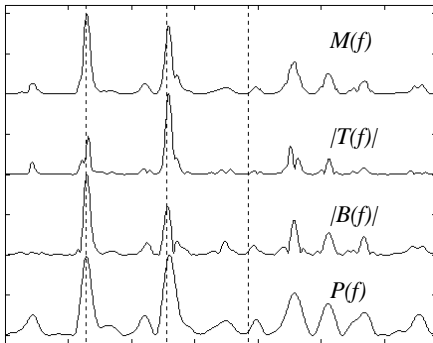


**Fig. 4.** Various spectrums of noised rectangular pulse train with  $tw=T/2$ . The estimated fundamental frequency is:  $fp=0.1807$ ,  $fb=0.1851$ ,  $ft=0.0614$ ,  $fm=0.0615$ .

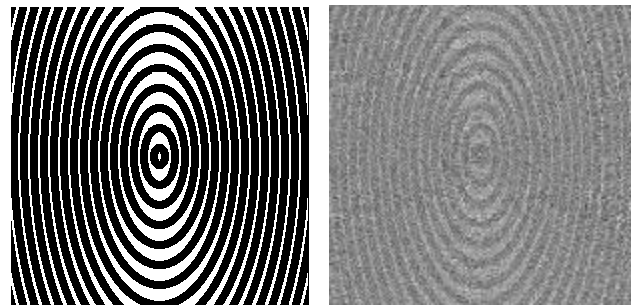
In Fig. 3 the maximal peak of power spectrum is located at the second harmonic due to the heavy noise. The trispectrum has a weak fundamental frequency component because the rectangular pulse train with pulse width of  $T/3$  has no third harmonic. Likewise, the maximal peak of bispectrum in Fig. 4 is located at the third harmonic due to the absence of the even harmonics of signal.

These two examples illustrate some problems of fundamental frequency estimation based on power

spectrum, bispectrum and trispectrum for an unknown, noised periodic non-sinusoidal signal. For a short duration of signal the noise is not strictly white. This may result in the maximal peak of power spectrum not located at the fundamental frequency. A periodic non-sinusoidal signal in the absence of even harmonics or third harmonic will have the bispectrum or trispectrum not working. These two examples have shown the mix-spectrum working well for unknown, noised, periodic non-sinusoidal signals.

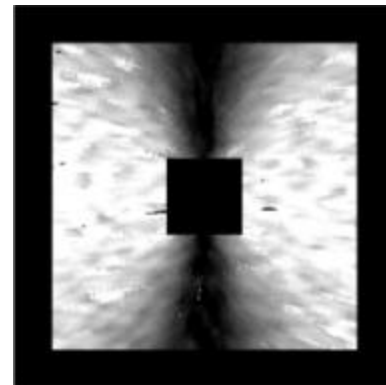
## 4. Experiments

Fig. 5 illustrates a synthetic image of size  $300 \times 300$  and its noised version (-6dB). The ridge frequency at each pixel is known (varying from  $1/20$  to  $1/10$ ).



**Fig. 5.** A synthetic image and its noised version.

The *x-signatures* were formed by using oriented windows of size  $33 \times 7$ . Ridge frequency was estimated by power spectrum, bispectrum, trispectrum and mix-spectrum. The mean square error of ridge frequency estimations at 54000 different pixels is  $[1.26, 0.65, 1.16, 0.31] \times 10^{-3}$  for power spectrum, bispectrum, trispectrum and mix-spectrum, respectively. The ridge frequency map obtained by the mix-spectrum is illustrated in Fig. 6.



**Fig. 6.** Ridge frequency map obtained by mix-spectrum.

Fig. 7 shows a sample fingerprint image and Fig. 8 illustrates its ridge frequency map obtained by the mix-spectrum. This ridge frequency map is full of bumps and holes due to the ridge discontinuities of the fingerprint image (ridge ending, bifurcation and scar).



Fig. 7. A sample fingerprint image.

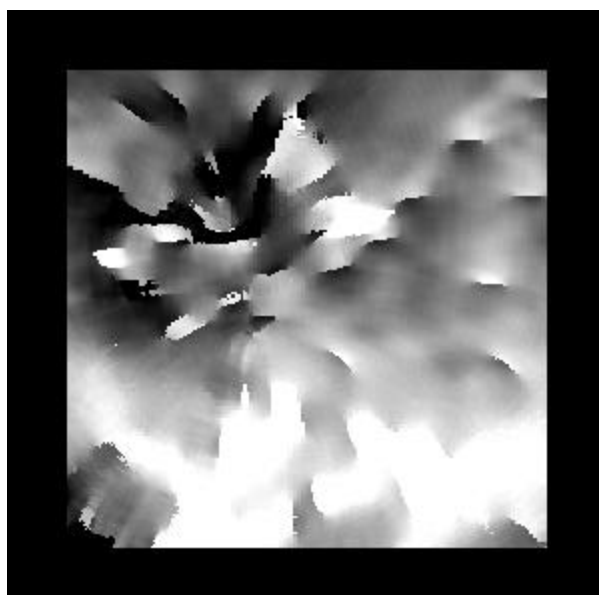


Fig. 8. The ridge frequency map of the fingerprint in Fig. 7 obtained by the mix-spectrum.

## 5. Conclusion

Fingerprint ridge frequency or ridgeline density is an intrinsic feature of a fingerprint image. The performance of applying various filters to the fingerprint image processing strongly relies on the accuracy of the ridge frequency estimation. Therefore, reliably estimating the ridge frequency is very useful for the effective processing of fingerprint images. The *x-signature* of ridges and valleys is usually not a sinusoidal-shape signal. For a

nonsinusoidal period signal its power is distributed to its fundamental frequency and harmonics. Due to the distribution of the signal power, the fundamental frequency component of the power spectrum may be much weaker than that of sinusoidal signal with the same power. Furthermore, the noise may have the harmonic components of power spectrum higher than the fundamental component. This will result in a false frequency estimation based on the power spectrum.

This work employed the mix-spectrum to enhance the fundamental frequency component by either the second or third harmonic. It works because the odd harmonics and the even harmonics cannot be zero at the same time for the signal of *x-signature* of ridges and valleys in practice. Furthermore, the mix-spectrum limits the enhancement of noise to some extent. The experimental studies showed the superiority of this technique for estimating the fingerprint ridge frequency comparing with the power spectrum, bispectrum and trispectrum.

## References

- [1] L. O'Gorman, J.V. Nickerson, "An approach to fingerprint filter design," *Pattern Recognition* 22 (1989) 29.
- [2] B.M. Mehre, "Fingerprint image analysis for automatic identification," *Mach. Vis. Appl.* 6 (1993) 124.
- [3] A.K. Jain, L. Hong, S. Pankanti, R. Bolle, "An identity-authentication system using fingerprints," *Proc. IEEE*, 85 (1997) 1365.
- [4] A.K. Jain, L. Hong, R. Bolle, "On-line fingerprint verification," *IEEE Trans. PAMI* 19 (1997) 302.
- [5] L. Hong, Y. Wan, A.K. Jain, "Fingerprint image enhancement: algorithm and performance evaluation," *IEEE Trans. PAMI* 20 (1998) 777.
- [6] D. Maio and D. Maltoni, "Ridge-line density estimation in digital images," *Proceedings 14<sup>th</sup> ICPR*, Brisbane (Australia), Aug. 1998, pages. 534-538.
- [7] C.L. Nikias and J.M. Mendel, "Signal processing with higher-order spectrum," *Signal Processing*, July 1993.
- [8] C.L. Nikias and M.R. Raghuveer, "Bispectrum estimation: a digital signal processing framework" *Proc. IEEE*, vol. 75, pages 869-891, 1987.
- [9] K.M. Hock "Narrowband weak signal detection by higher order spectrum," *IEEE Trans. Signal Processing* 44, pages 874-879, 1996.
- [10] X.D. Jiang, "Fundamental frequency estimation by higher order spectrum," *ICASSP 2000*, Istanbul (Turkey), June 2000.